

An Innovative Composite Reinforced with Bone-Shaped Short Fibers

Y. T. Zhu¹, J. A. Valdez¹, N. Shi², M. L. Lovato¹, M. G. Stout¹, S. J. Zhou³,
D. P. Butt¹, W. R. Blumenthal¹, and T. C. Lowe¹

¹Materials Science and Technology Division, MS G755

²Los Alamos Neutron Science Center, MS H805

³Applied Physics Division, MS B258

Los Alamos National Laboratory, Los Alamos, NM 87545

Scripta Materialia (in press), LAUR#97-4985

Introduction

Engineered composite materials are well known for their superior properties. For instance, fiber-reinforced composites have improved strength and stiffness over their unreinforced matrix. Short-fiber composites in particular have multiple advantages compared to those reinforced with long continuous filaments. They can be adapted to conventional manufacturing techniques, such as those used in powder metallurgy, casting, molding, drawing, extruding, machining, and welding (1-4). As a result, the cost to design and fabricate short-fiber composites is relatively low (5, 6). Short-fiber composites also can be made with relatively isotropic mechanical properties and can be easily molded into complex shapes (1), as required in some applications. These advantages have led to widespread applications of these composites in automobile, sporting goods and cutting tools industries (7, 8).

Obtaining optimum strength and toughness in short-fiber composites remains a challenge. The extensive world-wide effort to design and optimize properties of continuous fiber composites through control of fiber-matrix interfaces properties is not directly applicable to short-fiber composites. In fact, these interfaces play a critical role and, in many cases, become a limiting factor in improving mechanical properties (9-12). For a short fiber composite, a strong interface is desirable to transfer load from the matrix to the fibers. A stronger interface can increase the effective length of the fiber that carries load (13-15). However, with a strong interface it is difficult to avoid fiber breakage caused by fiber stress concentrations interacting with the stress field of an approaching crack (16, 17). This effect is particularly severe for ceramic matrix composites, because of their low matrix toughness and lack of plasticity. Even for composites with highly ductile matrices, such as plastics, strong interfaces may still cause successive breakage of adjacent fibers and reduce the composite toughness (9, 17). Although fracture toughness is enhanced by crack bridging in weakly bonded continuous filament composites this mechanism is limited in short-fiber composites because a weak interface significantly decreases the length of the fiber that carries load. Compromising interfacial bond strength in short-fiber composites may result in *complete* fiber interfacial debonding and pullout. This may produce a significant loss of the composite strength with only a minimal improvement in the composite toughness.

The key to optimizing short-fiber composite properties is to obtain both a weak interface and a strong load transfer mechanism from the matrix to the fiber. This can be achieved by modifying the morphology of short fibers. For example, a bone-shaped short fiber with two enlarged ends can effectively transfer load from matrix onto the fiber at both ends by matrix-fiber interlocking, hence minimizing the need for a strong interface to transfer load. As a result, crack bridging

across weakly bonded fibers, a concept from continuous filament composites, can be used in short-fiber composites. The enlarged ends help to reduce the fiber stress concentration at a matrix crack tip by allowing interface sliding/debonding without complete fiber pullout. This is rarely achievable in conventional short-fiber composites. Since load is transferred through mechanical interlocking between the enlarged fiber ends and the matrix, the load-carrying potential of short fibers can be better utilized. If the shape and size of the enlarged fiber ends can be optimized in such a way that the short fiber would be pulled out with difficulty, much more energy would be consumed during the crack propagation, which will significantly improve the toughness. These advantages should translate into significantly higher ultimate strength, and higher toughness for this class of bone-shaped short-fiber composites having weak-to-moderate interfacial adhesion.

To evaluate the above innovative concept, we developed a method to make a prototype bone-shaped short-fiber composite and measured its properties. The initial results show that the bone-shaped short-fiber composite has a much higher strength and, in some cases, higher toughness than the conventional short-fiber composite.

Experimental Procedure

For ease of processing, we chose a polymer based composite system: commercial polyethylene (Micro Dyneema™) fibers in a polyester matrix. Bone-shaped short fibers were fabricated using a jig designed in our laboratory and a small hydrogen torch. The jig assembly consisted of three matching multiple slotted metal plates. A continuous filament with a diameter of 181 μm was wrapped multiple times around one of the plates, which was later sandwiched between the two other matching plates. Then a precision hydrogen flame was passed through the length of the slots cutting the exposed filaments to lengths of 3.6 mm or 4.9 mm and leaving two enlarged ends on each fiber. Conventional short fibers without enlarged ends were also prepared using a pair of scissors.

To suspend the short fibers in the uncured polyester, 0.39 g of amorphous fumed silica (Cab-O-Sil, Cabot Corporation, Tuscola, Illinois) was added to 10 ml of polyester as a thickening agent before mixing with short fibers. The mixture of polyester and Cab-O-Sil was then run through repeated vacuum cycles to remove the air bubbles introduced during the mixing. 0.6 % by volume of Methyl Ethyl Ketone Peroxide (MERK hardener) and 0.5 g of short fibers were then added. The new mixture was again run through vacuum cycles to remove air bubbles. Finally, the mixture was extruded into a sample mold through a syringe. The sample mold produces a net-shaped sample for mechanical testing. The extrusion process aligns short fibers to some extent. Further alignment was obtained using the principle of elongation flow, which was achieved by sliding two mold parts against each other, forcing the mixture to flow in the longitudinal direction of the sample. The sample mold was then mounted onto a

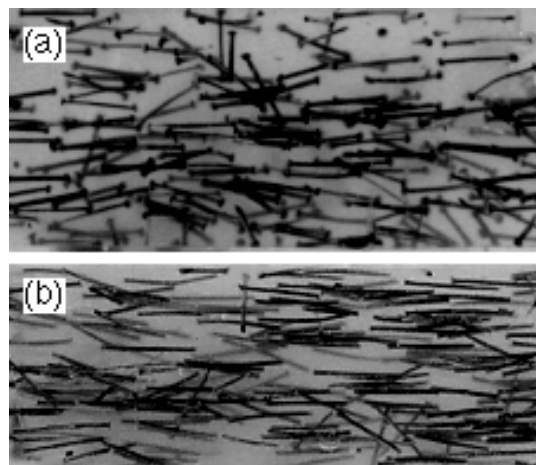


Fig. 1 Good fiber alignment was obtained in (a) bone-shaped and (b) conventional short-fiber composites

slowly rotating machine for four hours to prevent fibers from settling. Afterward, the samples were allowed to cure in air at room temperature for seven days before mechanical testing. Excellent fiber alignment and random fiber spatial-distribution were achieved using the above procedure (see Fig. 1).

Both bone-shaped and conventional short-fiber composite samples were fabricated using the procedure described above. The samples all had a fiber volume fraction of 5%. To study the effect of fiber length on the composite properties, fibers with two different lengths (3.6 and 4.9 mm) were used to reinforce the polyester matrix. Fiber-free blank matrix samples were also fabricated for comparison. Sample dimensions are shown in Fig. 2.

Tensile properties were measured using a Model 1125 Instron testing machine. An extensometer with an one inch gage length was used to measure the strain. A constant strain rate of 0.0001 s^{-1} was employed for all samples. Fracture surfaces were investigated using a JEOL 6300FXV Scanning Electron Microscope (SEM).

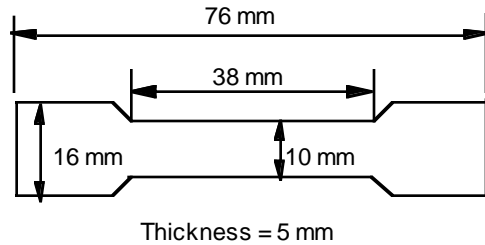


Fig. 2. The dimensions of composite tensile samples

Results and Discussion

The strain-stress curves of the bone-shaped and conventional short-fiber composites and matrix are shown in Fig. 3. The yield strengths were determined according to the ASTM standard D

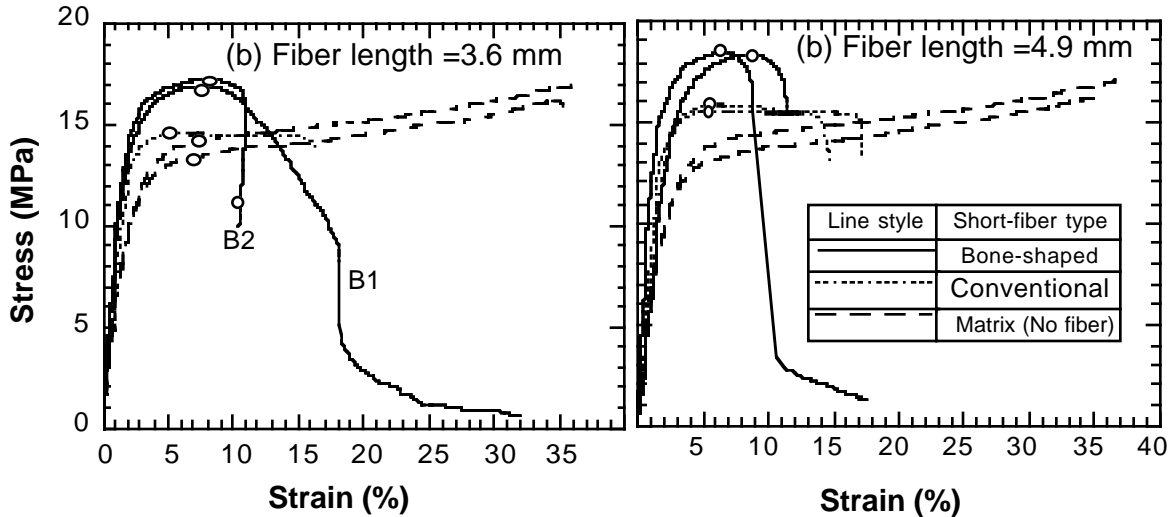


Fig. 3 Strain-stress curves of polyester matrix and composites reinforced with bone-shaped and conventional short fibers.

638M-91a. The circles on the strain-stress curves (Fig. 3a & b) indicate the measured yield strengths. Yield strengths of each sample are compared in Table I. The average strengths of the bone-shaped short fiber composites are greater than conventional short-fiber composites by 16.6 % and 17.0 % for samples with fiber lengths of 3.6 and 4.9 mm, respectively.

Table I. The yield strengths of the bone-shaped and conventional short fiber composites (fiber length $l = 3.6$ and 4.9 mm, respectively) and the polyester matrix.

Sample #	Bone-shaped (MPa)		Conventional (MPa)		Matrix (MPa)
	$l = 3.6$ mm	$l = 4.9$ mm	$l = 3.6$ mm	$l = 4.9$ mm	
1	17.26	18.45	14.65	15.86	14.20
2	16.90	18.36	—	15.60	13.40
Average	17.08	18.41	14.65	15.73	13.80

Table II compares the Young's moduli of the tensile samples. Young's modulus was determined from the slope of the strain-stress curve in the strain range of 0.2 to 1.1%. This range was chosen because the materials exhibited linear stress-strain behavior within it. On

average, the Young's modulus of the bone-shaped short-fiber composites is 18.4 % higher than the conventional short-fiber composites for samples with fiber length = 3.6 mm and 12.1% higher for samples with fiber length = 4.9 mm.

Table II. The Young's modulus of the bone-shaped and conventional short fiber composites and the polyester matrix.

Sample #	Bone-shaped (MPa)		Conventional (MPa)		Matrix (MPa)
	l = 3.6 mm	l = 4.9 mm	l = 3.6 mm	l = 4.9 mm	
1	778	668	689	670	566
2	853	1002	—	819	571
Average	816	835	689	745	569

Note that the fiber content in all composite samples is only 5%. The composite samples can be approximately considered as reinforced by unidirectional short fibers (see Fig. 1). Using a simple rule-of-mixture, the composite strength can be described as

$$\sigma_c = V_f \sigma_{ef} + (1 - V_f) \sigma_m \quad (1)$$

where σ_c is the yield strength of composites, V_f is the fiber volume fraction, σ_m is the average yield stress in matrix, σ_{ef} is the effective fiber stress at the composite yielding. The stress distribution along the fiber length is not uniform (18). For a conventional short fiber, σ_{ef} can be considered as the average stress along the fiber at composite yielding. For a bone-shaped short fiber, σ_{ef} is the average stress along the fiber, assuming the fiber length equals the volume of the fiber divided by its cross-section. This assumption slightly overestimates the actual fiber length because of the volume associated with the enlarged bone-shaped fiber ends. The effective stress at composite yielding can be calculated from Eq. 1 as

$$\sigma_{ef} = \left[\sigma_c - (1 - V_f) \sigma_m \right] / V_f \quad (2)$$

Using the average strength data from Table I, the effective fiber stress at composite yielding, σ_{ef} , is calculated and listed in Table III. It can be seen that the effective stress of bone-shaped fibers is 2.6 times of that of conventional fibers when the fiber length is 3.6 mm, and drops to 2.0 times when the fiber length is increased to 4.9 mm, which indicates that the difference in strengthening effectiveness between the bone-shaped short fibers and conventional short fibers decreases with increasing fiber length. On the other hand, the effective fiber stress increases with increasing fiber length for both types of composites. Note that with the same volume fraction, the bone-shaped short-fiber composite has fewer fibers per unit volume than conventional short-fiber composites because a bone-shaped short fiber has a larger volume than a conventional short fiber with the same length. Therefore, each bone-shaped short fiber is subject to higher effective stress than listed in Table III.

Toughness (energy consumed per unit volume of sample before failure) was calculated as the area under the stress-strain curve (19) using the equation:

$$\frac{Energy}{Volume} = \int_0^{\epsilon_f} \sigma d\epsilon \quad (3)$$

where ϵ_f is the failure strain. Table IV lists the toughness computed for each sample.

The toughness could not be calculated from curve B2. in Fig. 3a. This bone-shaped short-fiber composite, shows an unloading phenomenon before final failure because the sample didn't break in the gauge section. Otherwise, curve B2 would have looked like curve B1 in Fig. 3a, which is for the other bone-shaped short-fiber composite sample. It can be seen from Table IV that when

Table III. The effective fiber stress, σ_{ef}^b and σ_{ef}^s , for bone-shaped and conventional short-fiber composites, respectively, as calculated using Eq. 2

Fiber length	σ_{ef}^b	σ_{ef}^s	$\sigma_{ef}^s / \sigma_{ef}^b$
l = 3.6 mm	79.4	30.8	2.6
l = 4.9 mm	106.0	52.4	2.0

Table IV. Toughness of bone-shaped and conventional short fiber composites and the polyester matrix.

Sample #	Bone-shaped (KJ/m ³)		Conventional (KJ/m ³)		Matrix (KJ/m ³)
	l = 3.6 mm	l = 4.9 mm	l = 3.6 mm	l = 4.9 mm	
1	2763	1737	2197	2487	4897
2	—	1741	—	2094	5358
Average	2763	1739	2197	2291	5128

the fiber length is 3.6 mm, the toughness of bone-shaped short-fiber composites is 25% higher than that of the conventional short-fiber composites. However, when the fiber length is 4.9 mm, the toughness of bone-shaped short-fiber composites is 25% lower than that of the conventional short-fiber composites. As discussed in the introduction, if the fiber morphology can be optimized in such a way that much more energy would be consumed during the crack propagation due to difficult fiber pull-out, both the strength and the toughness of composite material will be significantly improved. This has been evidenced by the strain-stress curves of the bone shaped short fiber composites in which the fiber length is 3.6 mm (Fig. 3a). It is evident from curve B1 and B2 in Fig. 3a that the bone-shaped short fibers were effectively bridging cracks before sample failure, preventing an abrupt failure as in the conventional short-fiber composites. Note that toughness referred to above is very different from the fracture toughness, which is a measure of material resistance to crack propagation. We expect that the fracture toughness of bone-shaped short-fiber composites will be significantly higher than that of conventional short-fiber composites because the bone-shaped fibers can bridge cracks much more effectively.

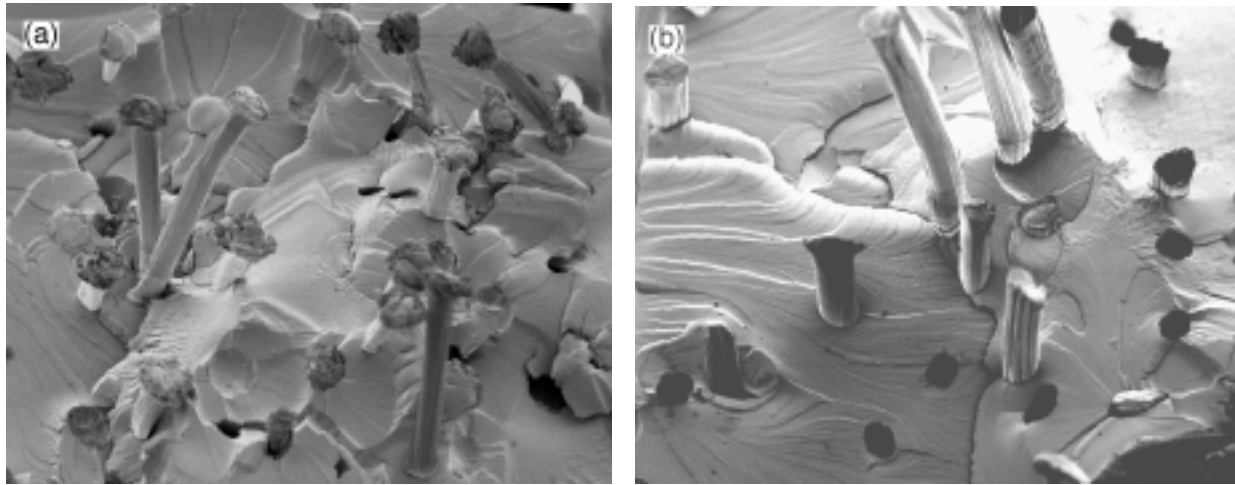


Fig. 4 SEM micrographs of fracture surfaces of (a) bone-shaped and (b) conventional short-fiber composites

SEM micrographs of fracture surfaces are shown in Fig. 4. It can be seen from Fig. 4a that many hackle marks radiate from fiber's ball ends or craters where the ball ends were before composite failure. This indicates that cracks were initiated at the balls, radiated out and later coalesced, resulting in the composite failure. Bone-shaped fibers extruding out of the fracture surface bridged the cracks before being pulled out. A closer look revealed that the fiber ends were disk-shaped and had relatively sharp edges. During the tensile testing, these edges create tensile stress concentration in the matrix that leads to crack formation. A smaller, elliptical fiber end with its long axis parallel to the fiber longitudinal direction will help to relieve the stress concentration and consequently further improve composite toughness. The fracture surface of a conventional short-fiber composite sample is shown in Fig. 4b, which clearly shows the pulled-out fibers and holes. Due to the weak interface, the fibers were easily pulled out, accounting for the observed lower yield strength and Young's modulus.

Conclusions

Using a model composite system, we have demonstrated the concept that bone-shaped short-fiber composites can yield both high strength and toughness, thus avoiding reliance on the interfacial properties as the limiting factor for improving the strength and toughness of short-fiber composites. The higher yield strength and Young's modulus of bone-shaped short fiber composites demonstrate that bone-shaped short fibers more effectively reinforce the composite matrix, most likely due to more effective crack bridging and load transfer.. Our results suggest that an optimized bone morphology, coupled with a weak interface, has the potential to significantly improve both the strength and toughness of short fiber composites. Further study is underway to optimize the fiber morphology to obtain the best combination of strength and toughness.

Acknowledgment

The authors acknowledge the support provided by the Laboratory Directed Research and Development Office of Los Alamos National Laboratory.

References

1. P. E. Chen, *Polymer Engineering and Science*, 11, 51 (1971).
2. P. K. Liaw, J. G. Gregg, and W. A. Logsdon, *J. Materials Science*, 22, 1613 (1987).
3. S. K. Gaggar and L. J. Broutman, *Polymer Engineering and Science*, 16, 537 (1976).
4. J. V. Milewski, *Concise Encyclopedia of Composite Materials*, revised edition, A. Kelly, Ed. p. 313, Elsevier Science, Ltd., Oxford, England (1994).
5. T. F. Klimowicz, *Journal of Metals*, November, p. 49 (1994).
6. Y. Takao, *Recent Advances in composites in the United States and Japan*, ASTM STP 864, J. R. Vinson and M. Taya, Eds. p. 685, American Society for Testing and Materials, Philadelphia (1985).
7. M. M. Schwartz, *Composite Materials Handbook*, 2nd ed, Chapter 7, p. 54, McGraw-Hill, Inc., New York (1992).
8. D. J. Bay, *Composite Applications*, T. J. Drozda, Ed. p. 3, Society of Manufacture Engineers, Dearborn, Michigan (1989).
9. A. Crasto, S. H. Own, and R. V. Subramanian, *Composite Interfaces*, H. Ishida and J. L. Koenig, eds., p. 133, Elsevier Science Publishers, New York (1986).
10. M. Fishkis, J. R. Yeh, and K. Wefers, *J. Materials Science*, 29, 110 (1994).
11. E. A. Feest, *Composites*, 25, 75 (1994).
12. S. M. Kunz, K. Chia, C. H. McMurtry, and W. D. G. Boecker, *Composite Applications*, T. J. Drozda, ed., p. 38, Society of Manufacture Engineers, Dearborn, Michigan (1989).
13. C. M. Friend, *Scripta Metall.*, 23, 33 (1989).
14. K. Xia and T. G. Langdon, *J. Materials Science*, 29, 5219 (1994).
15. Y. T. Zhu, G. Zong, A. Manthiram, and E. Eliezer, *J. Materials Science*, 29, 6281 (1994).
16. E. Yasuda, T. Akatsu, Y. Tanabe, and Y. Matsuo, *Composite Materials*, A. T. Benedetto, L. Nicolais, and R. Watanabe, eds., p. 167, Elsevier Science Publishers, New York (1992).
17. T. Norita, J. Matsui, and H. S. Matsuda, *Composite Interfaces*, H. Ishida and J. L. Koenig, eds., p. 123, Elsevier Science Publishers, New York (1986).
18. R. W. Hertzberg, *Deformation and Fracture Mechanics of Engineering Materials*, 3rd ed., p. 26, John Wiley & Sons, New York (1989).
19. Y. T. Zhu, W. R. Blumenthal, and T. C. Lowe, *J. Materials Science*, 32, 2037 (1997).